ENVIRONMENTAL ECONOMICS

2016 © The Authors, some rights reserved; exclusive licensee American Association for the Advancement of Science. Distributed under a Creative Commons Attribution NonCommercial License 4.0 (CC BY-NC).
10.1126/sciadv.1501026

Enhanced economic connectivity to foster heat stress–related losses

Leonie Wenz[1,2,3]* and Anders Levermann[1,2,4]*

Assessing global impacts of unexpected meteorological events in an increasingly connected world economy is important for estimating the costs of climate change. We show that since the beginning of the 21st century, the structural evolution of the global supply network has been such as to foster an increase of climate-related production losses. We compute first- and higher-order losses from heat stress–induced reductions in productivity under changing economic and climatic conditions between 1991 and 2011. Since 2001, the economic connectivity has augmented in such a way as to facilitate the cascading of production loss. The influence of this structural change has dominated over the effect of the comparably weak climate warming during this decade. Thus, particularly under future warming, the intensification of international trade has the potential to amplify climate losses if no adaptation measures are taken.

INTRODUCTION

An unabated increase of future greenhouse gas emissions will lead to a significant rise in global mean temperature (*1*) with severe impacts on natural and societal systems (*2*, *3*). Several studies, as reviewed by Dell *et al.* (*4*), focusing on the economic implications of changing climatic conditions suggest that weather fluctuations influence agricultural (*5*) and industrial (*6*) output, and the health (*7*, *8*) and energy (*9*) sectors, as well as exports of countries (*10*). They potentially amplify social conflicts (*11*, *12*) and migration (*13*). Although physiological heat stress is influenced by a number of meteorological factors (*14*), it has been shown that labor productivity declines quasilinearly with temperature above a threshold that is estimated to be ≥25°C (*15*–*22*). Reductions in labor supply associated with temperature shocks are observed mainly but not exclusively (*23*, *24*) in industries exposed to outdoor temperature, such as forestry, mining, and construction (*25*). In response to a global temperature rise, an increase in production losses due to heat stress can be expected if no adaptation measures are taken. At the same time, global market integration has increased economic linkages between countries. Production processes increasingly rely on (vertically integrated) supply chains spanning multiple countries and sectors (*26*, *27*). In a globally connected economy, a production reduction due to heat stress is not necessarily locally confined but can evoke supraregional repercussions through both the supply and the demand sides (*28*–*31*). It might entail further production reductions along the supply chain. Consequently, climate-related losses may be influenced by the structural evolution of the global economic network, which is subject to numerous nonclimatic factors. Here, we focus on this structural change and analyze how it relates to the cascading of production loss throughout the supply network. By (production) loss, we refer to a reduction in output of regional sectors [measured in U.S. dollars (USD) at day level] that can be induced by either diminished labor productivity due to heat stress (first-order loss) or associated changes in demand and supply [higher-order loss; as defined in Okuyama and Chang (*32*)].

There is a large body of economic literature on international trade [as reviewed by Donaldson (*33*) and Costinot and Rodriguez (*34*)], and the theoretical proposition that there are substantial benefits from market integration is very fundamental (*35*). For instance, empirical analyses suggest that facilitated resource allocation in past decades has led to efficiency gains in the U.S. agriculture sector in the same order of magnitude as the rate of technological progress (*36*) and has enhanced savings in global water resources (*37*); yet, beneficial short-term effects of trade might come along with reduced societal resilience in the long term (*38*). Trade dependencies can render countries vulnerable to adverse events in other parts of the world (*39*, *40*). For instance, it has been argued that global supply chains played a role in the 2009 global recession (*41*). Although, theoretically, trade has the potential to mediate the effects of supply shocks at comparably low costs (*36*, *42*), restricting trade policies were often applied in the past to stabilize domestic supply at the expense of market supply (*43*–*45*). Particularly in the light of increasingly frequent and intense extreme weather under future warming (*46*), a better understanding of the complex interdependencies in the network of global supply chains is required. Here, we provide a structural analysis of the economic network with respect to production failures in response to heat stress.

RESULTS

As a probing case, we combine data on temperature, population, and the global economic network at day level for the years 1991–2011 and analyze the economic system's susceptibility to heat stress–induced production losses and their propagation in each year. By susceptibility, we mean the magnitude of production losses that can potentially arise from heat stress throughout the network if only very basic response mechanisms and no economic adaptation are seized. These losses may be directly driven by the daily temperature (first order) or indirectly driven by the structure of economic dependencies within the network (higher order).

To this end, a population-weighted time series of daily mean temperature is computed for 186 countries using bias-corrected (*47*) observed temperature and population data on a 0.5° grid provided by the Inter-Sectoral Impact Model Intercomparison Project [ISI-MIP (*48*);

[1]Potsdam Institute for Climate Impact Research, 14473 Potsdam, Germany. [2]Institute of Physics, University of Potsdam, 14476 Potsdam, Germany. [3]Mercator Research Institute on Global Commons and Climate Change, 10829 Berlin, Germany. [4]Columbia University, New York, NY 10027, USA.
*Corresponding author. Email: leonie.wenz@pik-potsdam.de (L.W.); anders.levermann@pik-potsdam.de (A.L.)

Downloaded from http://advances.sciencemag.org/ on June 10, 2016

see Methods for more information]. As a representation of the global supply network, multi-regional input-output tables (MRIOTs) for the years 1991–2011 provided by the Eora MRIO database (*49*) are used. They represent annually averaged monetary transactions between 26 industry sectors (and final demand) of these 186 countries (confer tables S1 and S2 as well as Methods for detailed information). The input and output flows are interpreted as links in a network of regional sectors and final demand (*50*). The sum of all output flows of a regional sector yields its daily production level.

Following a recent econometric study (*16*), the effect of temperature on labor supply is computed proportional to the daily temperature above 27°C. As suggested by the data, the production of the sectors of construction, agriculture and fishing, and mining and quarrying is reduced by a factor of 0.6, 0.8, and 4.2%, respectively, for each degree above this threshold (table S1). Exemplary time series for the South Korean construction and the Ecuadorian agriculture sector (fig. S1) show the shock-like daily heat stress forcing on the production. Here, the analysis is restricted to these sectors because of their potential to induce higher-order losses. Sectors with potential gain from warming are not considered. The resulting reductions in production levels (in USD) are denoted first-order losses due to heat stress. The perturbation is only applied in countries located in a belt between 30°N and 30°S around the equator (Fig. 1A and table S2) because the econometric study is restricted to tropical countries. The main conceptual result reported is altered by neither this specification nor the precise value of the temperature threshold (see fig. S2).

To estimate higher-order production losses associated with heat stress, that is, reduced production of other regional sectors due to supply and demand relations, the first-order production losses are propagated with the numerical model Acclimate (Fig. 1, B and C) (*51*, *52*). The model attributes several basic economic features to all regional sectors in the network of economic flows and describes their dynamic interaction (see Methods for more detail). It propagates production losses from one regional sector to another through forward (supply shortages) and backward (demand reductions) linkages in the network. In case of supply shortages, the production of a regional sector

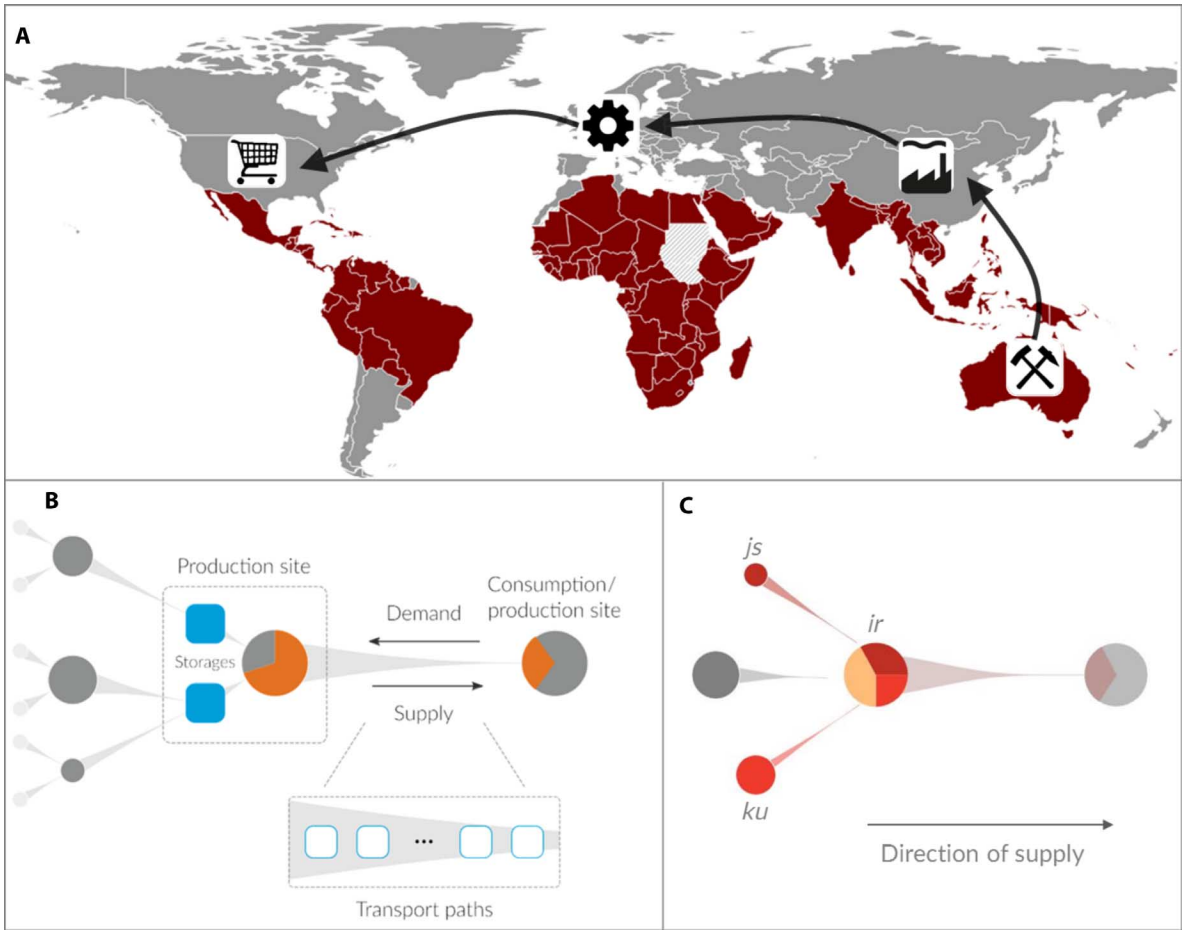

Fig. 1. Production loss propagation. (**A**) Basic setup of the study. Production reductions in the sectors of agriculture and fishing, mining and quarrying, and construction due to heat stress (measured in USD at day level) are computed for tropical countries (shaded in red). These first-order losses can induce production reductions in other regions and sectors (higher-order losses) through linkages in the global supply network. The cascading of production losses is simulated by use of the model Acclimate. (**B**) Schematic illustration of the model Acclimate. Production losses are passed on from one production site to another (or a consumption site) through demand and supply relations. Storage, transport time, and the possibility of demand redistribution can buffer the propagation. (**C**) Perfect complementarity as main nonlinearity of loss propagation. Production in regional sector *ir* is limited by the strongest relative failure of its suppliers (here, *js* and *ku* with $j \neq k$).

Downloaded from http://advances.sciencemag.org/ on June 10, 2016

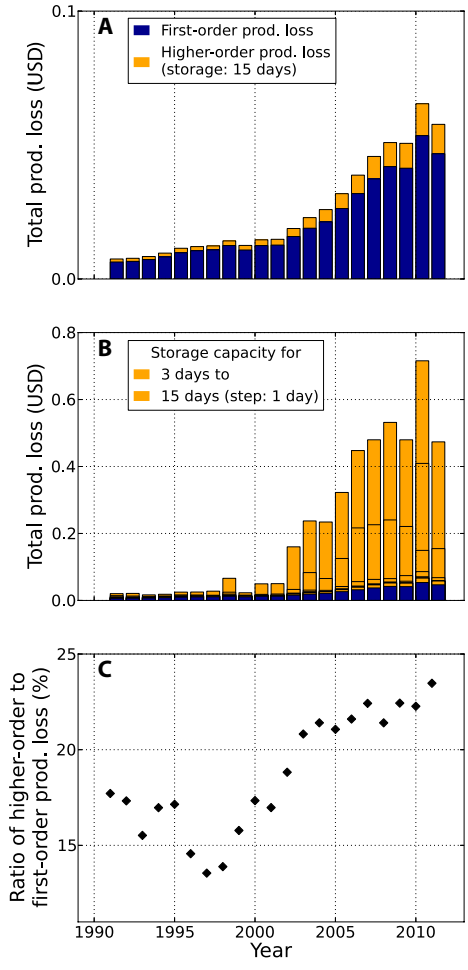

Fig. 2. Production losses change over time and the effect of higher-order losses is significant. (**A**) Decomposition of total production loss. Total production losses are composed of first- and higher-order losses that both increase over the simulation period (1991–2011). (**B**) Role of storage for loss propagation. Higher-order production losses vary with storage size (given in days of input volume; here, 3 to 15 days), but larger storage capacities can reduce higher-order production losses only to a certain extent. They saturate when above a storage size of about 10 days' worth of total input is reached. (**C**) Ratio of higher- to first-order production loss. Higher-order production losses are about 12 to 20% of first-order losses for storage capacities of 15 days.

is limited by the minimal relative availability of one input good across all input goods following the assumption of perfect complementarity; that is, if, for example, 10% of one input (and less of all other inputs) is missing, production is reduced by this factor. The loss propagation is buffered by the existence of storage, transport-induced time delay, and the possibility of demand redistribution.

The modeling framework used here purposefully differs from alternative approaches, such as static input-output (I-O) and computable general equilibrium (CGE) models, to capture the network-related economic response to perturbations on the same time scale as those occur. Static I-O and CGE models simulate the economic response to an exogenous shock at one specific point in time, and dynamic CGE models typically have coarse time steps of 1 to 10 years (*53*). By contrast, the dynamic framework applied here depicts the economic response at day level. This is central to the study because we do not analyze one major shock but small daily perturbations due to heat stress. Dynamic CGEs generally include an intertemporal optimization, thereby adapting a social planner's perspective that implies that the representative agents in these models have strong spatial oversight and perfect temporal foresight. Accordingly, shocks can be anticipated, the welfare-optimizing path of the system is sorted out, and economic losses are mitigated more effectively compared to the situation of unexpected perturbations that is considered here (*54*). Another difference to most CGEs is the more heterogeneous representation of the global economic system. Such heterogeneity is also reflected in static I-O models, but they have been criticized for overestimating economic losses from shocks (*31*, *53*). Because they assume a fixed production system, important mediating effects are ignored. Our approach attempts to find a middle ground in that it combines the heterogeneous perspective of I-O approaches with a more flexible economic system. The complex dynamics of loss propagation are modeled in a simplified framework that allows analyzing structural dependencies without neglecting some very basic buffering mechanisms such as storage, transport, and demand adjustments. The model Acclimate is designed in the spirit of an agent-based model with almost 5000 regional sectors as agents, which seek to regain their initial productivity as quickly as possible after a perturbation. They dynamically interact with their direct network neighbors to avoid production losses. However, these production losses are not expected by the regional sectors. After a perturbation, the model gradually strives back to its initial state as given by the data but is not constrained by the assumption of a general equilibrium of prices and quantities in each time step. Apart from CGEs,

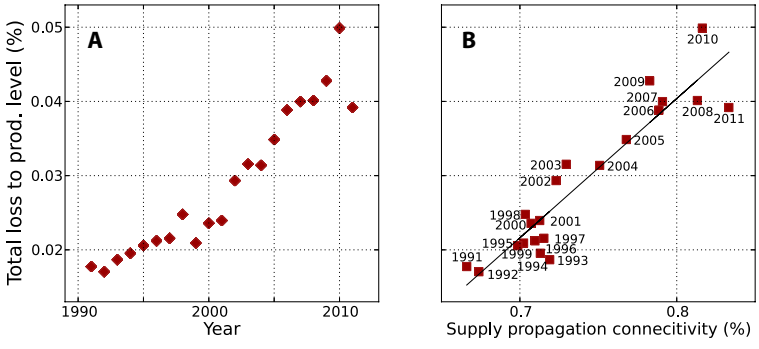

Fig. 3. Changes in network structure increase relative production loss. (**A**) Relative production losses in each simulation year. The ratio of total production loss to annual production level (in %) increases with time. (**B**) Relative production losses increase with the static network measure SPC. The static network measure SPC correlates with the losses in each year.

Downloaded from http://advances.sciencemag.org/ on June 10, 2016

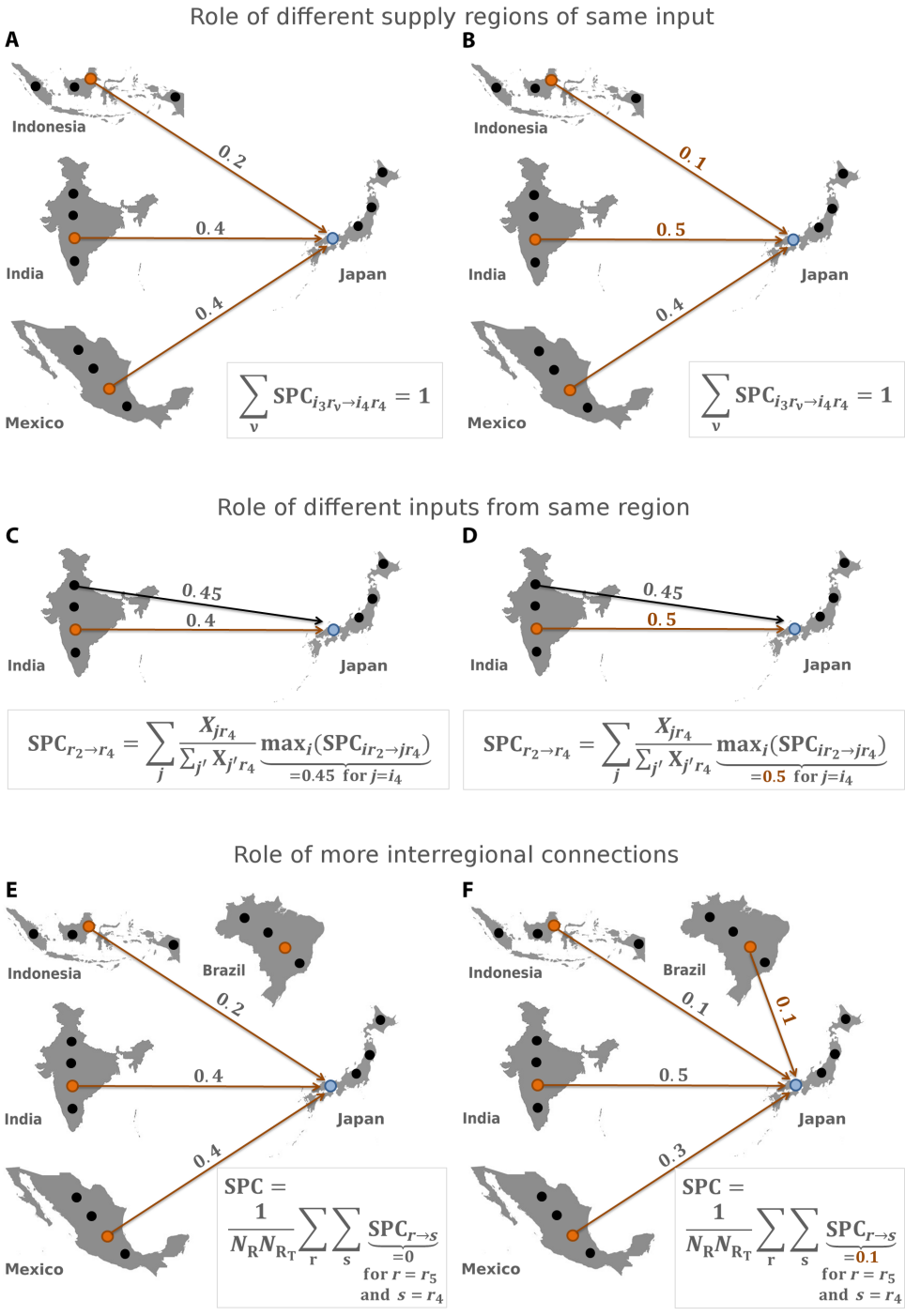

Fig. 4. Exemplary illustration of network measure SPC. (**A** and **B**) Role of different supply regions of the same input. In this simplified example, the fourth Japanese sector obtains the input good i_3 from three different tropical countries. The respective SPC values result from the share that each of these production sites has on the total supply of i_3 to the Japanese sector. These shares can change over time but always add up to 1. (**C** and **D**) Role of different inputs from the same region. The dependence of Japan on supplies from India is determined by the maximal sectoral impact that India has on each sector in Japan. (**E** and **F**) Role of enhanced interregional connectedness. The global average of all regional SPC values can change either because of new connections in the network or because the established link structure varies.

Downloaded from http://advances.sciencemag.org/ on June 10, 2016

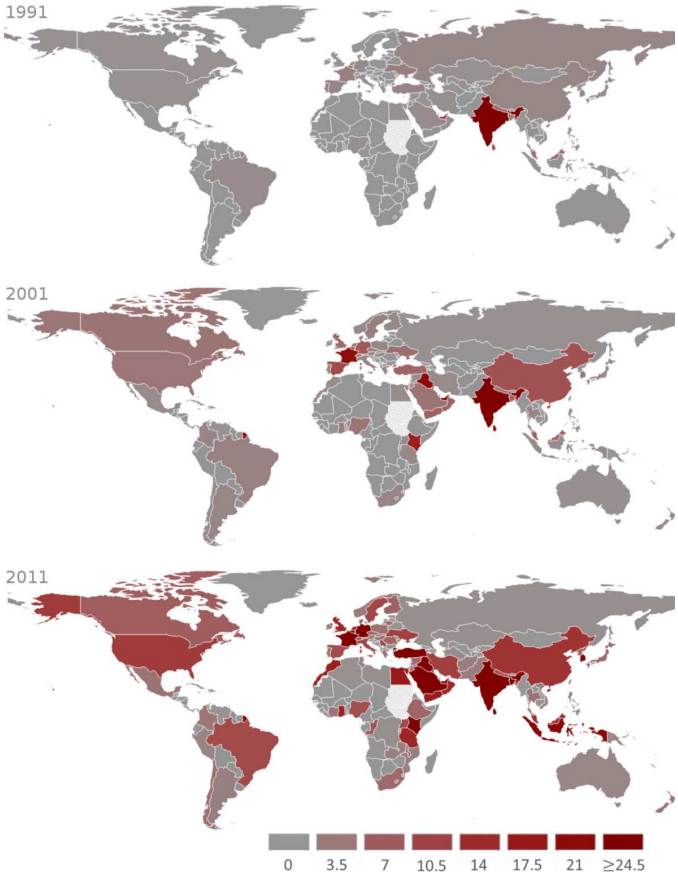

Fig. 5. Regional SPC for the case of India. (**A** to **C**) Maps show how dependent a country's production is on supplies from India according to the regional SPC values in 1991 (A), 2001 (B), and 2011 (C). Dark red color denotes that the dependency is equal to or larger than 24.5%.

gravity and Ricardian models (*55*) are often applied in trade theory to investigate the gains of and barriers to market integration. They are also general equilibrium approaches and often focus on trade patterns between few (often just two) countries, whereas the approach presented here aims to analyze the economic system's interaction at a global scale without the equilibrium assumption.

For each of the years 1991–2011, we compute the first-order production loss induced by heat stress, as described above. Then, we simulate the propagation of this loss with the numerical anomaly model Acclimate to account for higher-order losses throughout the network of economic flows.

The simulations indicate that total annual production losses from heat stress (that is, first- and higher-order losses in USD aggregated across sectors, regions, and days) are substantial and, in this century, increase with time (Fig. 2, A and B). A decomposition of total production loss shows that higher-order losses contribute significantly to the total loss (Fig. 2A). They vary in dependence on the size of storage, but even when very high storage capacities are assumed, higher-order losses arise (Fig. 2B). Above a saturation value, an increase in storage size does not considerably diminish higher-order losses. The results then become independent of the storage size. All analyses in this study use a storage size of 15 days well within the saturation range (as in Fig. 2A). In this case, higher-order losses are between 12 and 24% of the first-order losses (Fig. 2C).

We find that total annual production losses increase between 1991 and 2011. This trend is not as pronounced in the 1990s but becomes apparent from 2001 on. As a measure for this trend, but not to be taken as quantification of actual economic climate damages, the production loss value increases almost by an order of magnitude, that is, between 10 and 60 billion USD per year (Fig. 2A).

Because the temperature time series does not show a corresponding trend in the first decade of the 21st century (fig. S3), this difference is not climate-driven. Furthermore, it cannot solely be explained by economic growth because it is also seen in relative production losses,

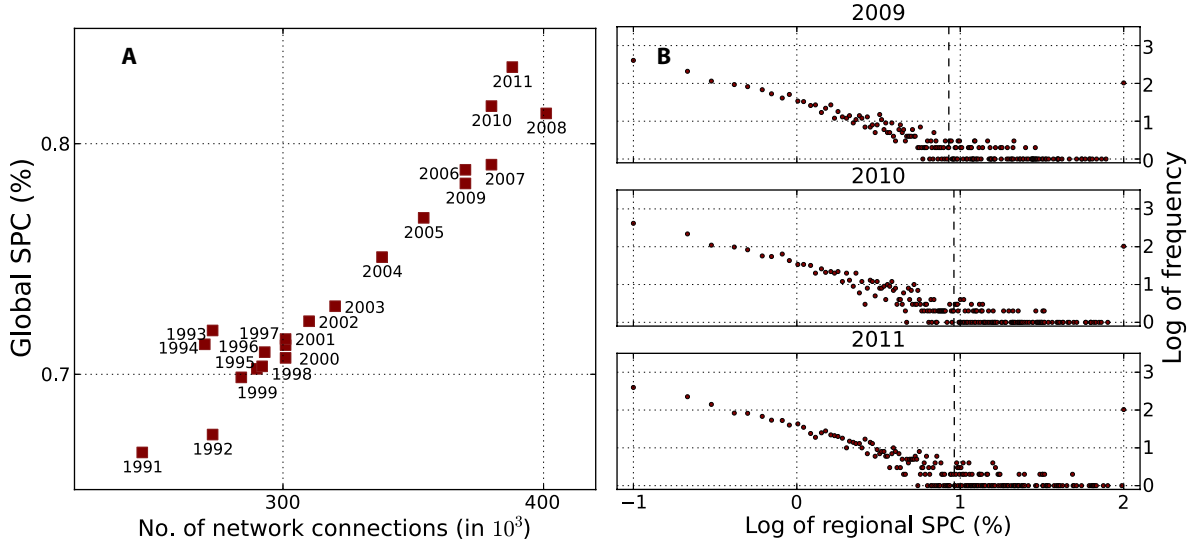

Fig. 6. Change of economic network's SPC over time. (**A**) Number of network connections. Global network measure SPC increases over time and is strongly correlated with the number of connections in the network. (**B**) Log-log frequency distribution of regional SPC values. The histogram of regional SCP values is shifted toward larger SCP values over time as represented by the mean (vertical dashed lines), suggesting that dependencies on supplies from tropical countries have become larger on average. The mean values for all years are given in fig. S5.

Downloaded from http://advances.sciencemag.org/ on June 10, 2016

that is, total production losses per year as a share of the global annual production level (Fig. 3A). Relative losses grow quasilinearly with the simulation year during this decade. Moreover, the contribution of higher-order losses to the total loss rises over time, whereas the contribution of first-order losses declines (fig. S4 and Fig. 2C). Consequently, the economic structure present in the different years that are underlying the simulations dominates the system's susceptibility to heat stress–induced production loss, and the recent evolution of the economic network has been such as to facilitate the propagation of losses; that is, the dynamic susceptibility is due to the static structure of the network.

To describe and analyze this relationship, a static network measure, the Supply Propagation Connectivity (SPC), is introduced. SPC is a globally and annually averaged network measure that determines the economic connectivity in terms of the dependence of production in different countries on supplies from other countries (see Methods for definition and Fig. 4 for a conceptual illustration). This static network measure correlates with the relative production losses caused by unexpected heat stress events in the respective years (Fig. 3B). It represents a change in the network structure that results in an increase in the economic system's susceptibility to production loss in the 1991–2011 period and particularly during the years 2001–2011 (see Fig. 5 for an illustration).

This correlation is nontrivial especially because the SPC measure is a global average of all regional SPC values (see Methods for detail). Its value can change over time either because the number of nonzero regional SPC values is changing or because the existing regional SPC values vary. The first effect is given by the link density of the supply network measured by the number of links over the number of possible links. This density has been steadily grown over the first decade of this century (*50*) and is dominating the change in the network's SPC (Fig. 6A). A smaller part of the change in global SPC is explained by quantitative changes in the strength of existing dependencies (Fig. 6B). The log-log frequency distribution of regional SPC values is shifted toward higher values over time, as represented by the mean (fig. S5), indicating that existing dependencies on supply from tropical countries have become larger.

DISCUSSION

The regional SPC is a ratio representing the dependence of production in one country on supplies from another country, which, in this study, is particularly a tropical one. We find that the global average of this ratio is a good predictor for global economic losses due to unexpected climatic events if no economic adaptation occurs, as what can be expected on the fast daily time scale considered here. This qualitative result is unlikely to depend on the specific representation of loss propagation within the model Acclimate because the characteristics of the propagation dynamics that are necessary for our results are very fundamental; that is, any other model of production loss propagation along the supply network is likely to show the same dependence on the network structure. Here, we find that global SPC was stagnant during the last decade of the previous century and that it steadily increased in the first decade of this century. We further find that this was mainly due to an increase in the number of network links. Whereas the losses found here are small in absolute terms, the increase that we find in the first decade of the century is significant. This suggests that the current evolution of the supply network might facilitate the propagation of climate-induced production losses.

As a thought experiment, we compute heat stress–induced production losses for a future scenario of unmitigated climate change without economic adaptation. To this end, we use economic data and population distribution for a fixed year between 1991 and 2011 (which we refer to as economic base year) and combine it with a time series of daily temperature data corresponding to the strongest warming scenario [Representative Concentration Pathway (RCP) 8.5 (*56*); see Methods for detail]. Total and relative annual production losses until 2100 vary again by an order of magnitude for the different economic base years (fig. S6). Although the specific values of the time series cannot be considered projections because they assume a fixed economic network without adaptation, the sensitivity of the losses to the economic structure is a robust feature of the simulations. It is thus likely that in a warming world, future changes in the complex global supply network will be a major factor in the evolution of the costs of climate change.

METHODS

Data

For this study, daily mean temperature data on a horizontal grid of 0.5° × 0.5° resolution from the ISI-MIP (*48*) climate data set were combined with coherent socioeconomic scenarios defined by population and economic data for the years 1991–2011.

Temperature data. For the analysis of the 1991–2011 period, we take data from the WFDEI (WATCH-Forcing-Data-ERA-Interim) meteorological forcing data set (*57*), where the WATCH Forcing Data methodology was applied to the ERA-Interim reanalysis data (*58*). Projections correspond to RCP 8.5 (*56*). They build on data by the Princeton Earth System Model of the Geophysical Fluid Dynamics Laboratory [GFDL-ESM2M (*59*)] of the Coupled Model Intercomparison Project Phase 5 [CMIP-5 (*60*)]. The application of a bias correction technique (*47*) ensures statistical agreement with historical observations of the WATCH database.

Population data. Population data on a 0.5° grid for the years 1991–2011 were also taken from the ISI-MIP data set. Population projections (from 2010 on) correspond to the second Shared Socioeconomic Pathway (*61*), and the historical information is derived from the United Nations World Population Prospects (UNWPP) national estimates.

Economic data. The economic network was constructed using data from the Eora26 World MRIO data set (*49*) covering annual monetary transactions between 26 industry sectors and final demand in 186 countries. For our computations, we used the MRIOTs in basic prices for the years 1991–2011 (version 199.324). Because small flows are more likely to be subjected to large balancing adjustments in the MRIOT generating process (*62*), each flow that contributed less than 1.6×10^{-6}% (in the order of 10^6 USD in 2001) to the global annual flow volume was neglected in the computation. Results reported in this study became even more pronounced for a fixed cutoff value of 10^6 USD for all simulation years (fig. S2C). For our simulation time step of one day, we divided the annual data by 365 to yield the average daily transactions.

Population-weighted temperature time series per country. For each country covered by the Eora World MRIO, a population-weighted time series of daily mean temperature was computed. To this

Downloaded from http://advances.sciencemag.org/ on June 10, 2016

end, a country mask provided by the Global Administrative Areas initiative (www.gadm.org/country) assigning grid cells to countries was used. Very small tropical countries were not captured by the mask. Given their comparably small contribution to the global production level, they were not considered in our analysis.

Model Acclimate

The model Acclimate is detailed in the Supplementary Materials as well as in extensive description papers (*51*, *52*). It builds on a network representation of the global supply network based on input-output matrices (*49*). The nodes in this network are production and consumption sites that are connected through input and, in case of a production site, output flows (in USD per day). The dynamics occur through decisions by these sites to avoid production losses. The model thereby operates on discrete time steps of 1-day length. It accounts for storage capacities and geographically derived transportation times. Production sites produce in accordance with the availability of inputs, the demand requests they receive, and, possibly, external perturbations (for example, as induced by meteorological events). They distribute their output among several customers and request inputs from different suppliers in dependence on their current storage level and under consideration of the recent reliability of each supplier. Inputs can either be immediately processed or be stored for later production. Production is limited by the assumption of perfect complementarity, that is, if one input is lacking by a certain percentage, the entire production is reduced by the same factor. The model adopts a Leontief production function with fixed coefficients and without substitution elasticities. The economic state, given by the annual data, serves as a baseline for the model. Its evolution over time is not modeled. Instead, the model simulates the response to an external perturbation (for example, heat stress) after which it strives back to this initial state. The external forcing is modeled as a production reduction that may be passed on from one production site to another through forward and backward linkages in the economic network. In the case of forward loss propagation, production sites experience a lack of inputs. They receive less demand requests in the case of backward loss propagation. Production sites cannot anticipate a perturbation, but respond to supply shortages or demand reductions by reverting to stored inputs by redirecting their demand to unaffected suppliers and by readjusting their production capacity. For this study, we used the following model setup: we assume that there are enough storage capacities to maintain production for 15 days without input (we also compare scenarios where storages can last for 3 to 15 days, respectively). This initial storage capacity can be surpassed by a factor of 2. If the storage level diminishes, demand is adjusted to regain half of the initial storage level within 5 days. Varying demand shares are requested from different suppliers with the aim of receiving inputs as fast as possible. Herein, past performances of suppliers, in decreasing shares, are taken into account, whereas no market forces are considered. The initial production capacity cannot be enhanced, and the network is not allowed to restructure. Although the model cannot claim to precisely depict real-world supply and demand dynamics, it represents the basic propagation of the effect of production reduction along the supply chains as required for this study.

Network measure SPC

SPC measures dependencies in the network of economic flows. It can be computed at different scales, that is, for production sites, regions, and the global network as a whole. In the context of this study, we primarily consider the global SPC value with respect to supplies from tropical countries. On the level of production sites, SPC is computed for each economic flow $Z_{ir \to js}$ from the input-output tables and expresses how dependent a production site $j \in \{1, \ldots, N_I\}$ in an arbitrary region $s \in \{1, \ldots, N_R\}$ is on supplies from any other production site i in a tropical region $r \in \{1, \ldots, N_{R_T}\}$

$$\mathrm{SPC}_{ir \to js} = \frac{Z_{ir \to js}}{\sum_{r'} Z_{ir' \to js}} \forall ir \neq js$$

where N_{R_T} denotes the number of tropical regions, N_R is the number of all regions, and N_I is the number of sectors. It is thereby an upper limit of the dependency mainly because it assumes that the supply is not compensated by enhanced productivity of other production sites and because it postulates perfect complementarity of the production process. On the regional level, SPC describes how dependent an arbitrary region s is on direct supplies from a tropical country r. It is computed by weighing the maximal sectoral impact r imposes on each sector j it supplies in region s by the ratio to which this production site contributes to the overall production $\sum_{j'} X_{j's}$ of region s and by summing up over all production sites j in region s

$$\mathrm{SPC}_{r \to s} = \sum_j \frac{X_{js}}{\sum_{j'} X_{j's}} \max_i \left(\mathrm{SPC}_{ir \to js}\right)$$

At the global scale, SPC is given by the mean of all regional SPC values

$$\mathrm{SPC} = \frac{1}{N_R N_{R_T}} \sum_r \sum_s \mathrm{SPC}_{r \to s}$$

It describes the general economic connectivity of the network in terms of production dependencies on supplies from tropical countries.

SUPPLEMENTARY MATERIALS

Supplementary material for this article is available at http://advances.sciencemag.org/cgi/content/full/2/6/e1501026/DC1

Description of the model Acclimate

fig. S1. Examples of forcing time series of first-order daily production loss due to heat stress.

fig. S2. Independence of main result on modeling assumptions.

fig. S3. Annually averaged global mean temperature over time.

fig. S4. Contribution of first-order and higher-order losses to total annual production loss.

fig. S5. Mean value from log-log histogram of regional SPC values.

fig. S6. Heat stress–induced production losses under the RCP 8.5 warming scenario for different economic structures over time.

table S1. Alphabetical list of all sectors used in simulations.

table S2. Alphabetical list of all countries used in simulations.

REFERENCES AND NOTES

1. T. F. Stocker, D. Qin, G.-K. Plattner, M. Tignor, S.K. Allen, J. Boschung, A. Nauels, Y. Xia, V. Bex, P.M. Midgley, *IPCC, 2013: Climate Change 2013: The Physical Science Basis. Contribution of Working Group I to the Fifth Assessment Report of the Intergovernmental Panel on Climate Change* (Cambridge Univ. Press, Cambridge, UK and New York, NY, USA, 2013), 1535 pp.
2. O. Edenhofer, R. Pichs-Madruga, Y. Sokona, *IPCC, 2014: Climate Change 2014: Mitigation of Climate Change. Working Group III Contribution to the Fifth Assessment Report of the*

Downloaded from http://advances.sciencemag.org/ on June 10, 2016

Intergovernmental Panel on Climate Change (Cambridge Univ. Press, Cambridge, UK and New York, NY, USA, 2014), 1086 pp.
3. C. B. Field, V. R. Barros, D. J. Dokken, K. J. Mach, M. D. Mastrandrea, T. E. Bilir, M. Chatterjee, K. L. Ebi, Y. O. Estrada, R. C. Genova, B. Girma, E. S. Kissel, A. N. Levy, S. MacCracken, P. R. Mastrandrea, L. L.White, *IPCC, 2014: Climate Change 2014: Impacts, Adaptation, and Vulnerability. Contribution of Working Group II to the Fifth Assessment Report of the Intergovernmental Panel on Climate Change* (Cambridge Univ. Press, Cambridge, UK and New York, NY, USA, 2014), pp. 1–32.
4. M. Dell, B. F. Jones, B. A. Olken, What do we learn from the weather? The new climate-economy literature. *J. Econ. Lit.* **52**, 740–798 (2014).
5. D. B. Lobell, W. Schlenker, J. Costa-Roberts, Climate trends and global crop production since 1980. *Science* **333**, 616–620 (2011).
6. M. Dell, B. F. Jones, B. A. Olken, Temperature shocks and economic growth: Evidence from the last half century. *Am. Econ. J. Macroecon.* **4**, 66–95 (2012).
7. J. A. Patz, D. Campbell-Lendrum, T. Holloway, J. A. Foley, Impact of regional climate change on human health. *Nature* **438**, 310–317 (2005).
8. F. Bosello, R. Roson, R. S. J. Tol, Economy-wide estimates of the implications of climate change: Human health. *Ecol. Econ.* **58**, 579–591 (2006).
9. M. Auffhammer, E. T. Mansur, Measuring climatic impacts on energy consumption: A review of the empirical literature. *Energy Econ.* **46**, 522–530 (2014).
10. B. F. Jones, B. A. Olken, *Climate Shocks and Exports* (National Bureau of Economic Research, Cambridge, MA, 2010), vol. 100, pp. 454–459.
11. S. M. Hsiang, M. Burke, E. Miguel, Quantifying the influence of climate on human conflict. *Science* **341**, 1235367 (2013).
12. M. B. Burke, E. Miguel, S. Satyanath, J. A. Dykema, D. B. Lobell, Warming increases the risk of civil war in Africa. *Proc. Natl. Acad. Sci. U.S.A.* **106**, 20670–20674 (2009).
13. R. McLeman, B. Smit, Migration as an adaptation to climate change. *Clim. Change* **76**, 31–53 (2006).
14. G. M. Budd, Wet-bulb globe temperature (WBGT)—Its history and its limitations. *J. Sci. Med. Sport* **11**, 20–32 (2008).
15. C. H. Wyndham, Adaptation to heat and cold. *Environ. Res.* **2**, 442–469 (1969).
16. S. M. Hsiang, Temperatures and cyclones strongly associated with economic production in the Caribbean and Central America. *Proc. Natl. Acad. Sci. U.S.A.* **107**, 15367–15372 (2010).
17. M. Dell, B. F. Jones, B. A. Olken, Temperature and income: Reconciling new cross-sectional and panel estimates. *Am. Econ. Rev.* **99**, 198–204 (2009).
18. T. Deryugina, S. M. Hsiang, *Does the Environment Still Matter? Daily Temperature and Income in the United States* (National Bureau of Economic Research, Cambridge, MA, 2014).
19. J. D. Ramsey, Task performance in heat: A review. *Ergonomics* **38**, 154–165 (1995).
20. O. Seppanen, W. J. Fisk, D. Faulkner, *Control of Temperature for Health and Productivity in Offices* (Lawrence Berkeley National Laboratory, Berkeley, CA, 2004).
21. J. J. Pilcher, E. Nadler, C. Busch, Effects of hot and cold temperature exposure on performance: A meta-analytic review. *Ergonomics* **45**, 682–698 (2002).
22. M. Burke, S. M. Hsiang, E. Miguel, Global non-linear effect of temperature on economic production. *Nature* **527**, 235–239 (2015).
23. G. P. Cachon, S. Gallino, M. Olivares, *Severe Weather and Automobile Assembly Productivity* (Columbia Business School Research Paper, New York, NY, 2012), 31 pp.
24. J. S. G. Zivin, S. M. Hsiang, M. J. Neidell, *Temperature and Human Capital in the Short- and Long-Run* (National Bureau of Economic Research, Cambridge, MA, 2015), 42 pp.
25. J. G. Zivin, M. Neidell, Temperature and the allocation of time: Implications for climate change. *J. Labor Econ.* **32**, 1–26 (2014).
26. A. Costinot, J. Vogel, S. Wang, An elementary theory of global supply chains. *Rev. Econ. Stud.* **80**, 109–144 (2012).
27. D. Hummels, J. Ishii, K.-M. Yi, The nature and growth of vertical specialization in world trade. *J. Int. Econ.* **54**, 75–96 (2001).
28. C. Kousky, Informing climate adaptation: A review of the economic costs of natural disasters. *Energy Econ.* **46**, 576–592 (2014).
29. A. van der Veen, Disasters and economic damage: Macro, meso and micro approaches. *Disaster Prev. Manag.* **13**, 274–279 (2004).
30. M. Christopher, H. Peck, Building the resilient supply chain. *Int. J. Logist. Manag.* **15**, 1–14 (2004).
31. Y. Okuyama, J. R. Santos, Disaster impact and input–output analysis. *Econ. Syst. Res.* **26**, 1–12 (2014).
32. Y. Okuyama, S. E. Chang, *Modeling Spatial and Economic Impacts of Disasters* (Springer, Berlin Heidelberg, 2004), 323 pp.
33. D. Donaldson, The gains from market integration. *Annu. Rev. Econ.* **7,** 619–647 (2015).
34. A. Costinot, A. Rodríguez-Clare, *Trade Theory with Numbers: Quantifying the Consequences of Globalization* (National Bureau of Economic Research, Cambridge, MA, 2013), 67 pp.
35. P. A. Samuelson, The gains from international trade once again. *Econ. J.* **72**, 820–829 (1962).
36. A. Costinot, D. Donaldson, C. B. Smith, *Evolving Comparative Advantage and the Impact of Climate Change in Agricultural Markets: Evidence from 1.7 Million Fields around the World* (National Bureau of Economic Research, Cambridge, MA, 2014), 45 pp.
37. C. Dalin, M. Konar, N. Hanasaki, A. Rinaldo, I. Rodriguez-Iturbe, Evolution of the global virtual water trade network. *Proc. Natl. Acad. Sci. U.S.A.* **109**, 5989–5994 (2012).
38. P. D'Odorico, F. Laio, L. Ridolfi, Does globalization of water reduce societal resilience to drought? *Geophys. Res. Lett.* **37**, L13403 (2010).
39. J. di Giovanni, A. A. Levchenko, Trade openness and volatility. *Rev. Econ. Stat.* **91**, 558–585 (2009).
40. C. Bren d'Amour, L. Wenz, M. Kalkuhl, J. C. Steckel, F. Creutzig, Teleconnected food supply shocks. *Environ. Res. Lett.* **11**, 35007 (2016).
41. J. Eaton, S. Kortum, B. Neiman, J. Romalis, *Trade and the Global Recession* (National Bureau of Economic Research, Cambridge, MA, 2011), 51 pp.
42. R. Burgess, D. Donaldson, Can openness mitigate the effects of weather shocks? Evidence from India's famine era. *Am. Econ. Rev.* **100**, 449–453 (2010).
43. T. Fellmann, S. Hélaine, O. Nekhay, Harvest failures, temporary export restrictions and global food security: The example of limited grain exports from Russia, Ukraine and Kazakhstan. *Food Secur.* **6**, 727–742 (2014).
44. W. Martin, K. Anderson, Export restrictions and price insulation during commodity price booms. *Am. J. Agr. Econ.* **94**, 422–427 (2012).
45. H. G. Jensen, K. Anderson, Grain price spikes and beggar-thy-neighbor policy responses: A global economywide analysis. *World Bank Econ. Rev.* 10.1093/wber/lhv047 (2015).
46. S. Rahmstorf, D. Coumou, Increase of extreme events in a warming world. *Proc. Natl. Acad. Sci. U.S.A.* **108**, 17905–17909 (2011).
47. S. Hempel, K. Frieler, L. Warszawski, J. Schewe, F. Piontek, A trend-preserving bias correction—The ISI-MIP approach. *Earth Syst. Dynam.* **4**, 219–236 (2013).
48. K. Frieler, A. Levermann, J. Elliott, J. Heinke, A. Arneth, M. F. P. Bierkens, P. Ciais, D. B. Clark, D. Deryng, P. Döll, P. Falloon, B. Fekete, C. Folberth, A. D. Friend, C. Gellhorn, S. N. Gosling, I. Haddeland, N. Khabarov, M. Lomas, Y. Masaki, K. Nishina, K. Neumann, T. Oki, R. Pavlick, A. C. Ruane, E. Schmid, C. Schmitz, T. Stacke, E. Stehfest, Q. Tang, D. Wisser, V. Huber, F. Piontek, L. Warszawski, J. Schewe, H. Lotze-Campen, H. J. Schellnhuber, A framework for the cross-sectoral integration of multi-model impact projections: Land use decisions under climate impacts uncertainties. *Earth Syst. Dynam.* **6**, 447–460 (2015).
49. M. Lenzen, K. Kanemoto, D. Moran, A. Geschke, Mapping the structure of the world economy. *Environ. Sci. Technol.* **46**, 8374–8381 (2012).
50. J. Maluck, R. V. Donner, A network of networks perspective on global trade. *PLOS One* **10**, e0133310 (2015).
51. R. Bierkandt, L. Wenz, S. N. Willner, A. Levermann, Acclimate—A model for economic damage propagation. Part 1: Basic formulation of damage transfer within a global supply network and damage conserving dynamics. *Environ. Syst. Decis.* **34**, 507–524 (2014).
52. L. Wenz, S. N. Willner, R. Bierkandt, A. Levermann, *Acclimate*—A model for economic damage propagation. Part II: A dynamic formulation of the backward effects of disaster-induced production failures in the global supply network. *Environ. Syst. Decis.* **34**, 525–539 (2014).
53. S. Hallegatte, Modeling the role of inventories and heterogeneity in the assessment of the economic costs of natural disasters. *Risk Anal.* **34**, 152–167 (2014).
54. J. D. Farmer, C. Hepburn, P. Mealy, A. Teytelboym, A third wave in the economics of climate change. *Environ. Resour. Econ.* **62**, 329–357 (2015).
55. J. Eaton, S. Kortum, Technology, geography, and trade. *Econometrica* **70**, 1741–1779 (2002).
56. D. P. van Vuuren, J. Edmonds, M. Kainuma, K. Riahi, A. Thomson, K. Hibbard, G. C. Hurtt, T. Kram, V. Krey, J.-F. Lamarque, T. Masui, M. Meinshausen, N. Nakicenovic, S. J. Smith, S. K. Rose, The representative concentration pathways: An overview. *Clim. Change* **109**, 5–31 (2011).
57. G. P. Weedon, S. Gomes, P. Viterbo, W. J. Shuttleworth, E. Blyth, H. Österle, J. C. Adam, N. Bellouin, O. Boucher, M. Best, Creation of the WATCH forcing data and its use to assess global and regional reference crop evaporation over land during the twentieth century. *J. Hydrometeorol.* **12**, 823–848 (2011).
58. D. P. Dee, S. M. Uppala, A. J. Simmons, P. Berrisford, P. Poli, S. Kobayashi, U. Andrae, M. A. Balmaseda, G. Balsamo, P. Bauer, P. Bechtold, A. C. M. Beljaars, L. van de Berg, J. Bidlot, N. Bormann, C. Delsol, R. Dragani, M. Fuentes, A. J. Geer, L. Haimberger, S. B. Healy, H. Hersbach, E. V. Hólm, L. Isaksen, P. Kållberg, M. Köhler, M. Matricardi, A. P. McNally, B. M. Monge-Sanz, J.-J. Morcrette, B.-K. Park, C. Peubey, P. de Rosnay, C. Tavolato, J.-N. Thépaut, F. Vitart, The ERA-Interim reanalysis: Configuration and performance of the data assimilation system. *Q. J. Roy. Meteorol. Soc.* **137**, 553–597 (2011).
59. J. P. Dunne, J. G. John, A. J. Adcroft, S. M. Griffies, R. W. Hallberg, E. Shevliakova, R. J. Stouffer, W. Cooke, K. A. Dunne, M. J. Harrison, J. P. Krasting, S. L. Malyshev, P. C. D. Milly, P. J. Phillipps, L. T. Sentman, B. L. Samuels, M. J. Spelman, M. Winton, A. T. Wittenberg, N. Zadeh, GFDL's ESM2 global coupled climate–carbon earth system models. Part I: Physical formulation and baseline simulation characteristics. *J. Climate* **25**, 6646–6665 (2012).
60. K. E. Taylor, R. J. Stouffer, G. A. Meehl, An overview of CMIP5 and the experiment design. *Bull. Am. Meteorol. Soc.* **93**, 485–498 (2012).
61. R. H. Moss, J. A. Edmonds, K. A. Hibbard, M. R. Manning, S. K. Rose, D. P. van Vuuren, T. R. Carter, S. Emori, M. Kainuma, T. Kram, G. A. Meehl, J. F. B. Mitchell, N. Nakicenovic, K. Riahi, S. J. Smith, R. J. Stouffer, A. M. Thomson, J. P. Weyant, T. J. Wilbanks, The next

Downloaded from http://advances.sciencemag.org/ on June 10, 2016

generation of scenarios for climate change research and assessment. *Nature* **463**, 747–756 (2010).
62. M. Lenzen, D. Moran, K. Kanemoto, A. Geschke, Building Eora: A global multi-region input–output database at high country and sector resolution. *Econ. Syst. Res.* **25**, 20–49 (2013).

Acknowledgments: We are grateful to S. Willner and C. Otto for their comments on the manuscript and their collaboration in the development of the model Acclimate. Map figures have been made using https://github.com/swillner/colour-map. We thank S. Hsiang for the very valuable input. **Funding:** This work was funded by the German Environmental Foundation and the European Union Seventh Framework Program FP7/2007-2013 under grant agreement no. 603864. The publication of this article was funded by the Open Access fund of the Leibniz Association. **Author contributions:** L.W. and A.L. designed the study and analyzed the results. L.W. conducted the analysis and led the writing of the paper. **Competing interests:** The authors declare that they have no competing interests. **Data and materials availability:** All data needed to evaluate the conclusions in the paper are present in the paper and/or the Supplementary Materials. Additional data related to this paper may be requested from the authors.

Submitted 1 August 2015
Accepted 18 May 2016
Published 10 June 2016
10.1126/sciadv.1501026

Citation: L. Wenz, A. Levermann, Enhanced economic connectivity to foster heat stress–related losses. *Sci. Adv.* **2**, e1501026 (2016).

Downloaded from http://advances.sciencemag.org/ on June 10, 2016

ScienceAdvances
AAAS

Enhanced economic connectivity to foster heat stress–related losses

Leonie Wenz and Anders Levermann (June 10, 2016)
Sci Adv 2016, 2:.
doi: 10.1126/sciadv.1501026

This article is publisher under a Creative Commons license. The specific license under which this article is published is noted on the first page.

For articles published under CC BY licenses, you may freely distribute, adapt, or reuse the article, including for commercial purposes, provided you give proper attribution.

For articles published under CC BY-NC licenses, you may distribute, adapt, or reuse the article for non-commerical purposes. Commercial use requires prior permission from the American Association for the Advancement of Science (AAAS). You may request permission by clicking here.

The following resources related to this article are available online at http://advances.sciencemag.org. (This information is current as of June 10, 2016):

Updated information and services, including high-resolution figures, can be found in the online version of this article at:
http://advances.sciencemag.org/content/2/6/e1501026.full

Supporting Online Material can be found at:
http://advances.sciencemag.org/content/suppl/2016/06/07/2.6.e1501026.DC1

This article **cites 50 articles,**8 of which you can be accessed free:
http://advances.sciencemag.org/content/2/6/e1501026#BIBL

Downloaded from http://advances.sciencemag.org/ on June 10, 2016

Science Advances (ISSN 2375-2548) publishes new articles weekly. The journal is published by the American Association for the Advancement of Science (AAAS), 1200 New York Avenue NW, Washington, DC 20005. Copyright is held by the Authors unless stated otherwise. AAAS is the exclusive licensee. The title Science Advances is a registered trademark of AAAS

Science Advances

AAAS

advances.sciencemag.org/cgi/content/full/2/6/e1501026/DC1

Supplementary Materials for

Enhanced economic connectivity to foster heat stress–related losses

Leonie Wenz and Anders Levermann

Published 10 June 2016, *Sci. Adv.* **2**, e1501026 (2016)
DOI: 10.1126/sciadv.1501026

The PDF file includes:

- Description of the model acclimate
- fig. S1. Examples of forcing time series of first-order daily production loss due to heat stress.
- fig. S2. Independence of main result on modeling assumptions.
- fig. S3. Annually averaged global mean temperature over time.
- fig. S4. Contribution of first-order and higher-order losses to total annual production loss.
- fig. S5. Mean value from log-log histogram of regional SPC values.
- fig. S6. Heat stress–induced production losses under the RCP 8.5 warming scenario for different economic structures over time.
- table S1. Alphabetical list of all sectors used in simulations.
- table S2. Alphabetical list of all countries used in simulations.

Supplementary Materials

Description of the model *acclimate*

The numerical model *acclimate* (*51*, 5*2*) describes the propagation of climate-induced production losses along global supply chains. It builds on a network representation of intra- and interregional economic relationships. The nodes in this network are production and consumption sites that are linked by input and output flows (in USD per day) derived from annual multi-regional input-output matrices (*49*). The total number of production and consumption sites is hence given by the data (in this study: 186 regions and 27 industry sectors including final demand, i.e. about 5000 sites). To explain the main mechanisms of the model, we here focus on an exemplary production site represented by the index pair js where j denotes the good being produced and s the region the site is located in. It is connected to other production sites ir and ku via input ($Z^*_{ir\to js}$) and output flows ($Z^*_{js\to ku}$).

The economic state given by the data serves as a baseline for the model (marked by the index *) whose evolution over time is not explicitly modeled. Instead the model simulates the response to small perturbations (here: daily production losses due to heat-stress) after which it strives back to this initial state. It operates on discrete time steps of length $\Delta t = 1\ \mathrm{day}$ thereby introducing dynamics on the input-output flows.

The model accounts for geographically-motivated transit times $\tau_{ir\to js}$ that are required to transport a good i from a region r to a production site js. The transport stock, i.e. total amount of good i from region r that is being transported to production site js at time step $(t+1)$, is given by

$$T^{(t+1)}_{ir\to js} = \sum_{b=0}^{\tau_{ir\to js}-1} Z^{(t+1-b)}_{ir\to js} \cdot \Delta t$$

All goods i arriving at production site js at time step $(t+1)$ add up to the total input flow $I^{(t+1)}_{i\to js}$ that is stored in an input-storage. The initial content $S^*_{i\to js} = \psi_i \cdot I^*_{i\to js}$ of this input-storage is a multiple of the initial input flow $I^*_{i\to js}$, where the parameter ψ_i expresses for how many days a production site can keep its production up if input i is lacking. The storage content $S^{(t+1)}_{i\to js}$ at time $(t+1)$ can exceed this initial content at most by a factor ω_i. It equals $S^{(t)}_{i\to js}$ unless the amount $U^{(t)}_{i\to js}$ of good i that was taken from the storage for production in the last time step differs from the number of inputs at that time:

$$S^{(t+1)}_{i\to js} = \max\left(\min\left(\omega_i \cdot S^*_{i\to js},\quad S^{(t)}_{i\to js} + \Delta t\left(I^{(t)}_{i\to js} - U^{(t)}_{i\to js}\right)\right),\quad 0\right)$$

Without an external perturbation, production site js uses its current inputs for production. In case the amount of inputs is not sufficient, it reverts to its input-storages. The possible use flow $\widehat{\mathrm{U}}_{\mathrm{i}\to\mathrm{js}}^{(\mathrm{t}+1)}$ of good i at time $(\mathrm{t}+1)$is hence given by

$$\widehat{\mathrm{U}}_{\mathrm{i}\to\mathrm{js}}^{(\mathrm{t}+1)} = \mathrm{I}_{\mathrm{i}\to\mathrm{js}}^{(\mathrm{t}+1)} + \frac{\mathrm{S}_{\mathrm{i}\to\mathrm{js}}^{(\mathrm{t}+1)}}{\Delta\mathrm{t}}$$

The maximum amount of output js can produce at time $(\mathrm{t}+1)$ is determined by the inputs that are available then, i.e. $\widehat{\mathrm{U}}_{\mathrm{i}\to\mathrm{js}}^{(\mathrm{t}+1)}$of all intermediate input goods i. The model thereby relies on the assumption of perfect complementarity which means that the minimum of the relative availability of one input good across all input goods determines the maximum relative productivity. The possible production ratio $\hat{\mathrm{p}}_{\mathrm{js}}^{(\mathrm{t}+1)}$ of js at time $(\mathrm{t}+1)$ that may also be limited to $\lambda_{\mathrm{js}}^{(\mathrm{t}+1)} \in [0,1]$ through an external perturbation reads

$$\hat{\mathrm{p}}_{\mathrm{js}}^{(\mathrm{t}+1)} = \min\left(\min_{\mathrm{i}}\left(\frac{\widehat{\mathrm{U}}_{\mathrm{i}\to\mathrm{js}}^{(\mathrm{t}+1)}}{\mathrm{U}_{\mathrm{i}\to\mathrm{js}}^{*}}\right), \qquad \lambda_{\mathrm{js}}^{(\mathrm{t}+1)}\right)$$

The actual production of js is determined not only by the availability of its intermediate inputs and a potential external forcing (possible production ratio $\hat{\mathrm{p}}_{\mathrm{js}}^{(\mathrm{t}+1)}$) but also by the demand requests it has received in the last time step (target production ratio $\tilde{\mathrm{p}}_{\mathrm{ku}}^{(\mathrm{t}+1)}$).

The demand $\mathrm{D}_{\mathrm{j}\leftarrow\mathrm{ku}}^{(\mathrm{t})}$ of any other production site, ku, for product j at time (t) is determined as follows: As long as the input-storage content (including all goods j that are being transported to ku at that time) remains constant, $\mathrm{D}_{\mathrm{j}\leftarrow\mathrm{ku}}^{(\mathrm{t})}$ equals the target use flow $\widetilde{\mathrm{U}}_{\mathrm{j}\to\mathrm{ku}}^{(\mathrm{t})}$ of product j at that time. This flow $\widetilde{\mathrm{U}}_{\mathrm{j}\to\mathrm{ku}}^{(\mathrm{t})}$ reflects the amount of good j that was or would have been necessary in order to fulfill all demand requests in that time step considering the imposed forcing $\lambda_{\mathrm{ku}}^{(\mathrm{t})}$. Otherwise, the demand is set such as to balance the difference. If the storage has decreased, the demand is increased in order to refill the storage within a certain time-frame regulated by the parameter γ_{j}. If by contrast the storage content has increased because the production site ku has not used all its inputs j, the demand decreases. Accordingly, $\mathrm{D}_{\mathrm{j}\leftarrow\mathrm{ku}}^{(\mathrm{t})}$ is given by

$$\mathrm{D}_{\mathrm{j}\leftarrow\mathrm{ku}}^{(\mathrm{t})} = \max\left(\widetilde{\mathrm{U}}_{\mathrm{j}\to\mathrm{ku}}^{(\mathrm{t})} + \frac{\left(\mathrm{S}_{\mathrm{j}\to\mathrm{ku}}^{*} + \sum_s \mathrm{T}_{\mathrm{js}\to\mathrm{ku}}^{*} - \mathrm{S}_{\mathrm{j}\to\mathrm{ku}}^{(\mathrm{t})} - \sum_s \mathrm{T}_{\mathrm{js}\to\mathrm{ku}}^{(\mathrm{t})}\right)}{\gamma_{\mathrm{j}}}, \qquad 0\right)$$

with $\widetilde{\mathrm{U}}_{\mathrm{j}\to\mathrm{ku}}^{(\mathrm{t})} = \tilde{\mathrm{p}}_{\mathrm{ku}}^{(\mathrm{t})} \cdot \lambda_{\mathrm{ku}}^{(\mathrm{t})} \cdot \mathrm{U}_{\mathrm{j}\to\mathrm{ku}}^{*}$.

Once a production site ku has determined its demand for good j, it distributes it among its respective suppliers considering how reliable each supplier has been, in diminishing shares weighted by the parameter $\varphi \in]0,1]$, in the last time steps. Production site js thus receives the following demand request from ku at time (t):

$$\mathrm{D}_{\mathrm{js}\leftarrow\mathrm{ku}}^{(\mathrm{t})} = \frac{\theta_{\mathrm{js}\rightarrow\mathrm{ku}}^{(\mathrm{t})} \cdot \mathrm{Z}_{\mathrm{js}\rightarrow\mathrm{ku}}^{*}}{\sum_{s'} \theta_{\mathrm{js}'\rightarrow\mathrm{ku}}^{(\mathrm{t})} \cdot \mathrm{Z}_{\mathrm{js}'\rightarrow\mathrm{ku}}^{*}} \cdot \mathrm{D}_{\mathrm{j}\leftarrow\mathrm{ku}}^{(\mathrm{t})}$$

with

$$\theta_{\mathrm{js}\rightarrow\mathrm{ku}}^{(\mathrm{t})} = \varphi \cdot \theta_{\mathrm{js}\rightarrow\mathrm{ku}}^{(\mathrm{t}-1)} + (1-\varphi) \cdot \vartheta_{\mathrm{js}\rightarrow\mathrm{ku}}^{(\mathrm{t})}$$

and

$$\vartheta_{\mathrm{js}\rightarrow\mathrm{ku}}^{(\mathrm{t})} = \frac{\mathrm{Z}_{\mathrm{js}\rightarrow\mathrm{ku}}^{(\mathrm{t})}}{\mathrm{D}_{\mathrm{js}\leftarrow\mathrm{ku}}^{(\mathrm{t}-1)}}$$

The sum of all demand requests $\mathrm{D}_{\mathrm{js}\leftarrow\mathrm{ku}}^{(\mathrm{t})}$ that js receives from different purchasers ku at time (t) determines its target production ratio $\tilde{\mathrm{p}}_{\mathrm{js}}^{(\mathrm{t}+1)}$ in the next time step:

$$\tilde{\mathrm{p}}_{\mathrm{js}}^{(\mathrm{t}+1)} = \frac{\sum_{\mathrm{k}} \sum_{\mathrm{u}} \mathrm{D}_{\mathrm{js}\leftarrow\mathrm{ku}}^{(\mathrm{t})}}{\mathrm{X}_{\mathrm{js}}^{*}}$$

where $\mathrm{X}_{\mathrm{js}}^{*} = \sum_{k} \sum_{\mathrm{u}} \mathrm{Z}_{\mathrm{js}\rightarrow\mathrm{ku}}^{*} = \sum_{k} \sum_{\mathrm{u}} \mathrm{D}_{\mathrm{js}\leftarrow\mathrm{ku}}^{*}$ denotes its initial production. The production ratio then reads

$$\mathrm{p}_{\mathrm{js}}^{(\mathrm{t}+1)} = \min\left(\tilde{\mathrm{p}}_{\mathrm{js}}^{(\mathrm{t}+1)}, \quad \hat{\mathrm{p}}_{\mathrm{js}}^{(\mathrm{t}+1)}\right)$$

and the total production is given by

$$\mathrm{X}_{\mathrm{js}}^{(\mathrm{t}+1)} = \mathrm{p}_{\mathrm{js}}^{(\mathrm{t}+1)} \cdot \mathrm{X}_{\mathrm{js}}^{*}$$

This output is then distributed equally among all purchasers:

$$\mathrm{Z}_{\mathrm{js}\rightarrow\mathrm{ku}}^{(\mathrm{t}+1)} = \frac{\mathrm{D}_{\mathrm{js}\leftarrow\mathrm{ku}}^{(\mathrm{t})}}{\sum_{k'} \sum_{\mathrm{u}'} \mathrm{D}_{\mathrm{js}\leftarrow\mathrm{k}'\mathrm{u}'}^{(\mathrm{t})}} \cdot \mathrm{X}_{\mathrm{js}}^{(\mathrm{t}+1)}$$

A consumption site $\mathrm{j_f s}$ is a slightly modified production site. Analogously, it has input storages and addresses demand requests. Unlike production, consumption is however not limited by the

assumption of perfect complementarity. Therefore, the total amount of good i that a consumption site $j_f s$ consumes at time $(t+1)$ is given by

$$C_{i\to j_f s}^{(t+1)} = U_{i\to j_f s}^{(t+1)} = c_{i\to j_f s}^{(t+1)} \cdot U_{i\to j_f s}^{*}$$

where the consumption ratio $c_{i\to j_f s}^{(t+1)}$ reads

$$c_{i\to j_f s}^{(t+1)} = \min\left(\frac{\widehat{U}_{i\to j_f s}^{(t+1)}}{U_{i\to j_f s}^{*}}, \qquad \lambda_{i\to j_f s}^{(t+1)}\right)$$

Figures and Tables

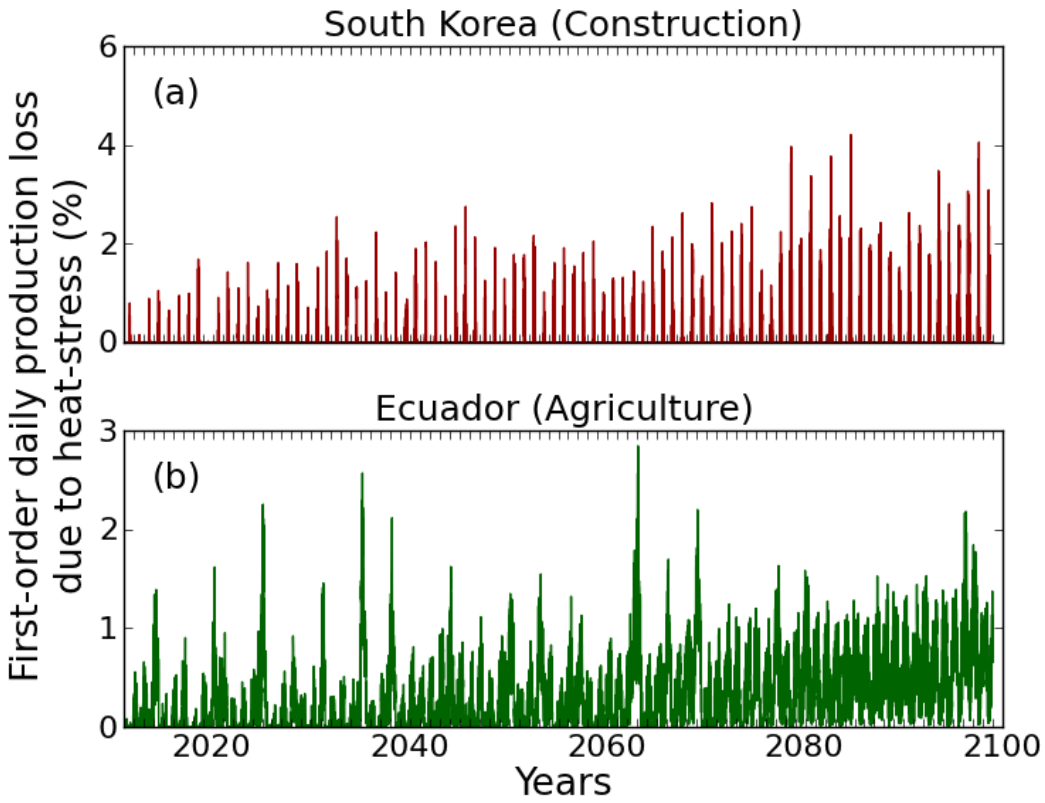

fig. S1. Examples of forcing time series of first-order daily production loss due to heat stress. Following econometric observations, daily economic output of the South Korean construction **(Panel a)** and the Ecuadorian agriculture **(Panel b)** sectors is reduced by 0.8 and 0.6%, respectively, for each additional degree above 27°C. This imposes a shock-like forcing upon the production of these regional sectors (exemplified here for the economic base year 2011). For most of the study only observed temperatures between the years 1991 and 2011 were used. Here we show the projections under the climate-change scenario RCP-8.5 in order to illustrate the future trend in the forcing.

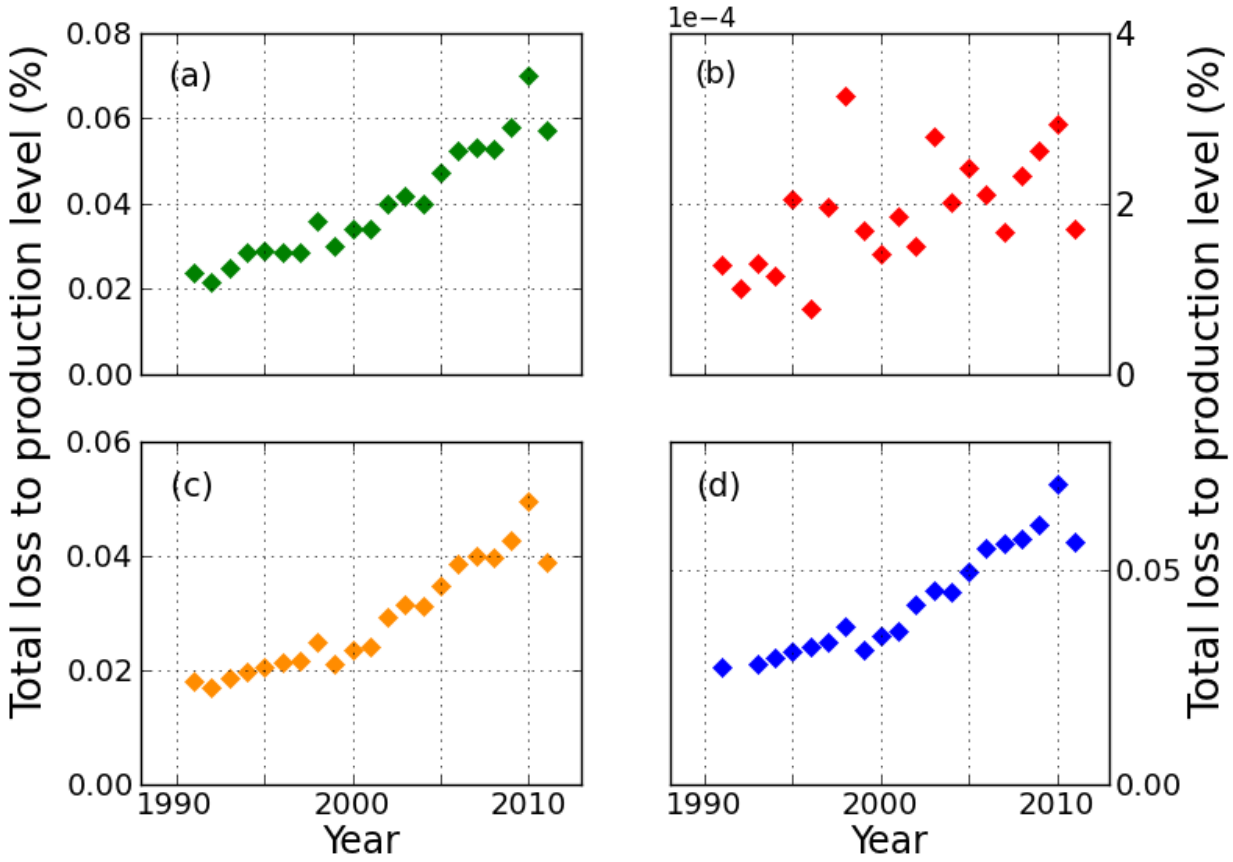

fig. S2. Independence of main result on modeling assumptions. Relative production losses under different scenarios increase over time. **Panel a: Heat-stress in all countries.** The relationship of temperature to labor productivity is not only applied to tropical countries but to all countries (186 in total). **Panel b: Heat-stress in the Caribbean and Central America.** The relationship of temperature to labor productivity is applied to countries in the Caribbean and Central America only (19 in total). **Panel c: Heat-stress in the tropics with fixed cut-off threshold for economic flows.** Very small flows from the annual input-output data are not filtered according to a variable threshold relative to the total flow volume in that year but according to a fixed threshold of 1 M USD (per year). **Panel d: Heat-stress in the tropics for temperature above 26°C.** It is assumed that the relationship of temperature to labor productivity already holds for temperature above 26°C instead of 27°C.

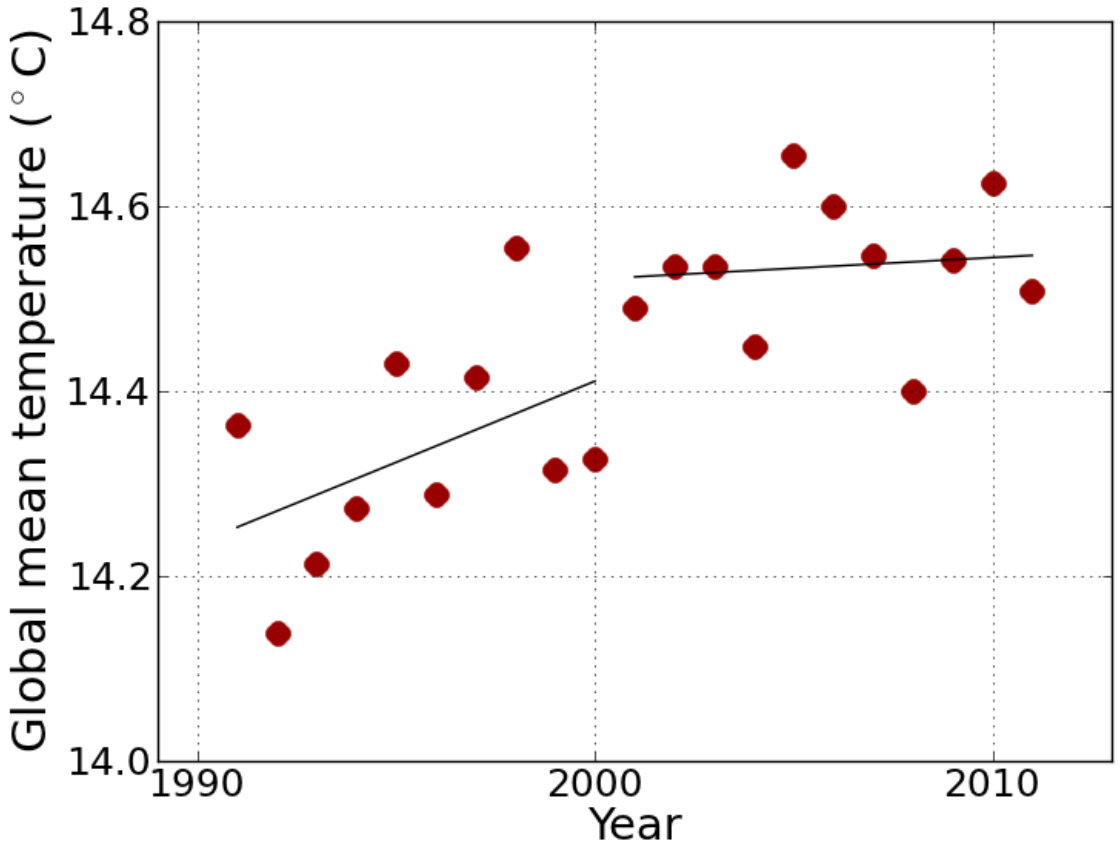

fig. S3. Annually averaged global mean temperature over time. Observation-based time series of annually averaged global mean temperature shows a trend in the 1991-2000-period but no trend in in the 2001-2011-period. Here, the time series of the WFDEI meteorological forcing data set (*57*) where the WATCH forcing data methodology was applied to ERA-interim reanalysis data (*58*) were used.

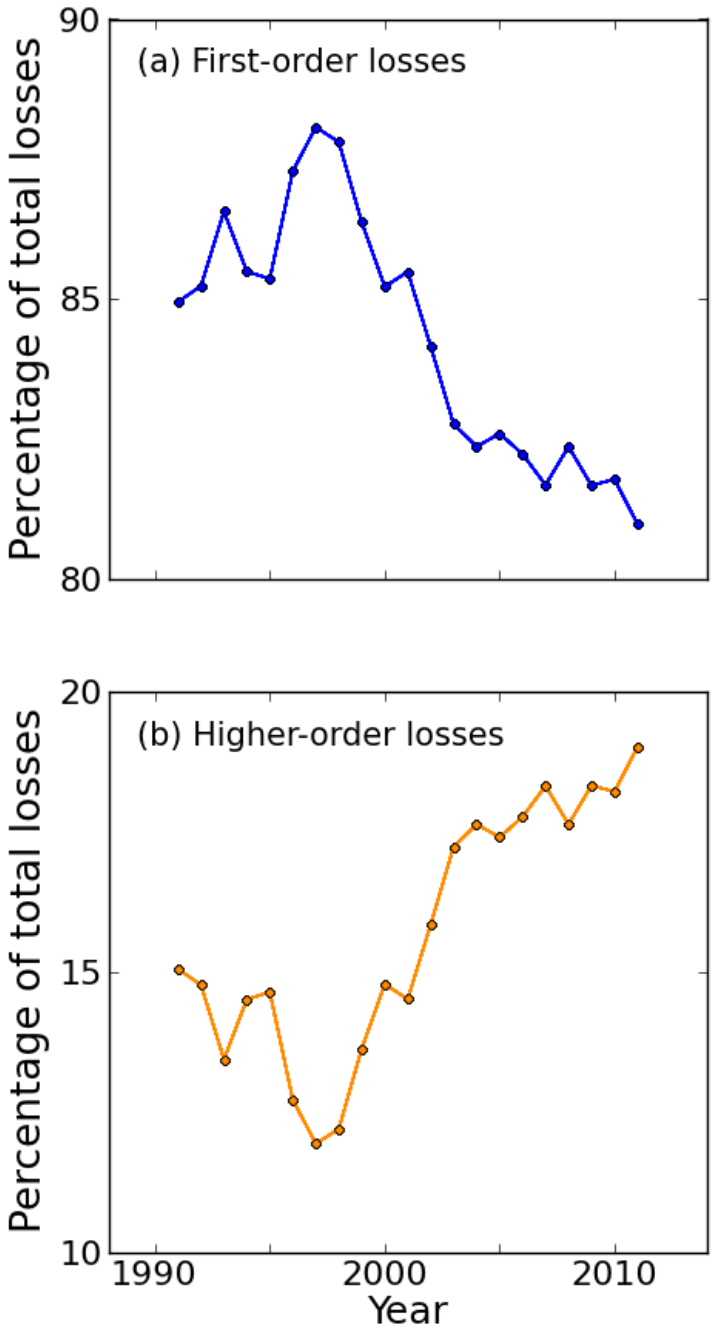

fig. S4. Contribution of first-order and higher-order losses to total annual production loss. *First-order losses* denote heat-stress-induced reductions in output of regional sectors (where the initial production level is given by multi-regional input-output data; compare Fig. 1). They can induce further productions reductions (*higher-order losses*) through linkages in the global supply network. The sum of all first- and higher-order losses per year yields the total loss in that year. While the share of first-order production losses as a percentage of total losses declines from 2001 on (Panel a), that of higher-order production losses increases (Panel b).

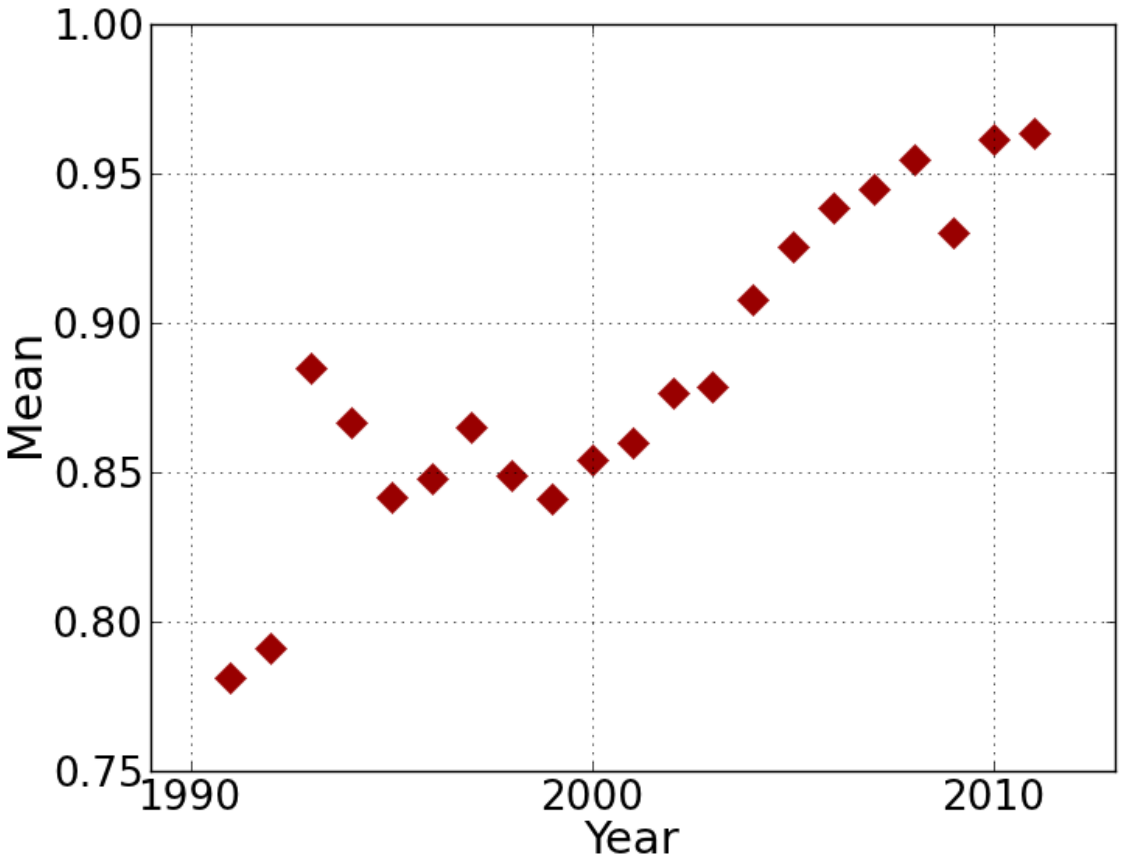

fig. S5. Mean value from log-log histogram of regional SPC values. Mean value of log-log frequency distribution of regional SPC values (Fig. 6B) increases over time. While the trend is not as clear in the 1990s, it becomes evident from 2001 on indicating that the distribution has been shifted towards higher values over time.

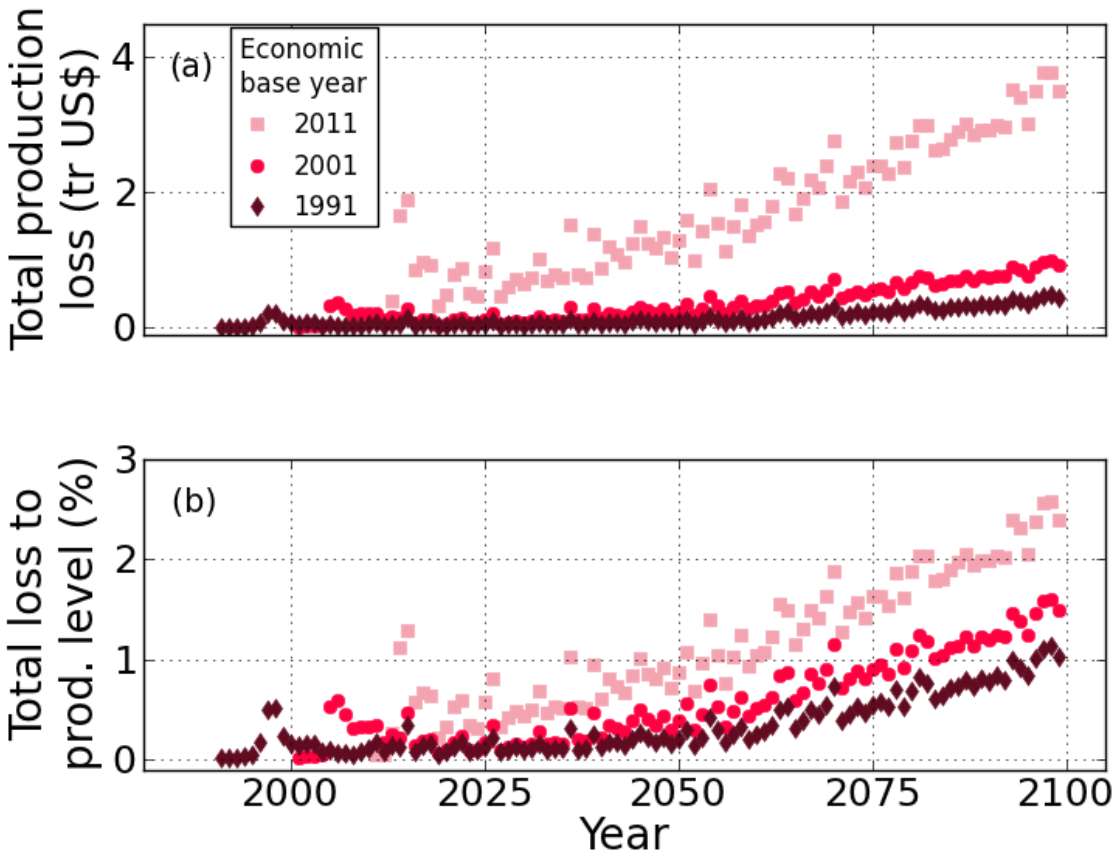

fig. S6. Heat-stress-induced production losses under the RCP 8.5 warming scenario for different economic structures over time. **Panel a: Total production losses.** Total production losses increase over time for different economic base years (here: 1991, 2001 and 2011) of the economic structure. **Panel b: Relative production losses.** Annual production losses as a share of total annual production increase over time for different economic base years.

table S1. Alphabetical list of all sectors used in simulations. Grey background denotes that the sector is assumed to be subjected to heat-stress in tropical countries. The percentage by which the output is reduced for each additional degree above 27°C is given in brackets.

Agriculture (0.8%)	Transport Equipment	Transport
Fishing (0.8%)	Other Manufacturing	Post and Telecommunications
Mining and Quarrying (4.2%)	Recycling	Financial Intermediation and Business Activities
Food & Beverages	Electricity, Gas and Water	Public Administration
Textiles and Wearing Apparel	Construction (0.6%)	Education, Health and Other Services
Wood and Paper	Maintenance and Repair	Private Households
Petroleum, Chemical and Non-Metallic Mineral Products	Wholesale Trade	Others
Metal Products	Retail Trade	Re-export & Re-import
Electrical and Machinery	Hotels and Restraurants	Final Demand

table S2. Alphabetical list of all countries used in simulations. Grey background denotes that countries are predominantly located in a belt between 30°N and 30°S around the equator. Very small tropical countries, as e.g. Aruba, were not captured by the temperature mask. Given their comparably minor contribution to the overall production level, they are not considered when computing the effects of heat-stress.

Afghanistan	Cambodia	French Polynesia	Latvia	Niger	South Africa
Albania	Cameroon	Gabon	Lebanon	Nigeria	Spain
Algeria	Canada	Gambia	Lesotho	Norway	Sri Lanka
Andorra	Cap Verde	Georgia	Liberia	Palestine	Suriname
Angola	Cayman Islands	Germany	Libya	Oman	Swaziland
Antigua and Barbuda	Central African Republic	Ghana	Liechtenstein	Pakistan	Sweden
Argentina	Chad	Greece	Lithuania	Panama	Switzerland
Armenia	Chile	Greenland	Luxembourg	Papua New Guinea	Syria
Aruba	China	Guatemala	Macao	Paraguay	Taiwan
Australia	Colombia	Guinea	Madagascar	Peru	Tajikistan
Austria	PR Congo	Guyana	Malawi	Philippines	Thailand
Azerbaijan	Costa Rica	Haiti	Malaysia	Poland	Macedonia
Bahamas	Croatia	Honduras	Maldives	Portugal	Togo
Bahrain	Cuba	Hong Kong	Mali	Qatar	Trinidad and Tobago
Bangladesh	Cyprus	Hungary	Malta	South Korea	Tunisia
Barbados	Czech Republic	Iceland	Mauritania	Moldova	Turkey
Belarus	Côte d'Ivoire	India	Mauritius	Romania	Turkmenistan
Belgium	North Corea	Indonesia	Mexico	Russia	Uganda
Belize	DR Congo	Iran	Monaco	Rwanda	Ukraine
Benin	Denmark	Iraq	Mongolia	Samoa	United Arab Emirates
Bermuda	Djibouti	Ireland	Montenegro	San Marino	United Kingdom
Bhutan	Dominican Republic	Israel	Morocco	Sao Tomé and Príncipe	Tanzania
Bolivia	Ecuador	Italy	Mozambique	Saudi Arabia	United States of America
Bosnia and Herzegovina	Egypt	Jamaica	Myanmar	Senegal	Uruguay
Botswana	El Salvador	Japan	Namibia	Serbia	Uzbekistan
Brazil	Eritrea	Jordan	Nepal	Seychelles	Vanuatu
British Virgin Islands	Estonia	Kazakhstan	Netherlands	Sierra Leone	Venezuela
Brunei	Ethiopia	Kenya	Netherlands Antilles	Singapore	Vietnam
Bulgaria	Fiji	Kuwait	New Caledonia	Slovakia	Yemen
Burkina Faso	Finland	Kyrgyzstan	New Zealand	Slovenia	Zambia
Burundi	France	Laos	Nicaragua	Somalia	Zimbabwe